DEVELOPMENTAL BIOLOGY

Huwe1-Mediated Ubiquitylation of Dishevelled Defines a Negative Feedback Loop in the Wnt Signaling Pathway

Reinoud E. A. de Groot,[1*] Ranjani S. Ganji,[2*] Ondrej Bernatik,[2,3] Bethan Lloyd-Lewis,[4†] Katja Seipel,[4‡] Kateřina Šedová,[5,6] Zbyněk Zdráhal,[5,6] Vishnu M. Dhople,[7] Trevor C. Dale,[4] Hendrik C. Korswagen,[1§] Vitezslav Bryja[2,3§]

Wnt signaling plays a central role in development, adult tissue homeostasis, and cancer. Several steps in the canonical Wnt/β-catenin signaling cascade are regulated by ubiquitylation, a protein modification that influences the stability, subcellular localization, or interactions of target proteins. To identify regulators of the Wnt/β-catenin pathway, we performed an RNA interference screen in *Caenorhabditis elegans* and identified the HECT domain–containing ubiquitin ligase EEL-1 as an inhibitor of Wnt signaling. In human embryonic kidney 293T cells, knockdown of the EEL-1 homolog Huwe1 enhanced the activity of a Wnt reporter in cells stimulated with Wnt3a or in cells that overexpressed casein kinase 1 (CK1) or a constitutively active mutant of the Wnt co-receptor low-density lipoprotein receptor–related protein 6 (LRP6). However, knockdown of Huwe1 had no effect on reporter gene expression in cells expressing constitutively active β-catenin, suggesting that Huwe1 inhibited Wnt signaling upstream of β-catenin and downstream of CK1 and LRP6. Huwe1 bound to and ubiquitylated the cytoplasmic Wnt pathway component Dishevelled (Dvl) in a Wnt3a- and CK1ε-dependent manner. Mass spectrometric analysis showed that Huwe1 promoted K63-linked, but not K48-linked, polyubiquitination of Dvl. Instead of targeting Dvl for degradation, ubiquitylation of the DIX domain of Dvl by Huwe1 inhibited Dvl multimerization, which is necessary for its function. Our findings indicate that Huwe1 is part of an evolutionarily conserved negative feedback loop in the Wnt/β-catenin pathway.

INTRODUCTION

In the canonical Wnt signaling pathway, the stability of the Wnt pathway effector β-catenin is regulated by a destruction complex, composed of the adenomatous polyposis coli protein (APC), Axin, casein kinase 1 (CK1), and glycogen synthase kinase 3β (GSK3β), which phosphorylates β-catenin and targets it for β-transducin repeat–containing protein (β-TrCP)–dependent ubiquitylation and proteasomal degradation. Binding of Wnt to the receptors Frizzled (Fz) and low-density lipoprotein receptor–related protein 6 (LRP6) leads to inhibition of destruction complex function and accumulation of β-catenin. β-Catenin can translocate to the nucleus and interact with members of the T cell factor/lymphoid enhancer factor (TCF/LEF) family of transcription factors to induce target gene expression (*1*).

The binding of Wnt to Fz and LRP6 induces clustering of the two receptors with the cytoplasmic protein Dishevelled (Dvl) into signalosomes at the plasma membrane (*2*). Dvl plays a key role during these upstream events in Wnt pathway activation. Upon Wnt stimulation, Dvl is phosphorylated by CK1ε (*3*, *4*) and Axin is recruited into the Dvl complex. Subsequent phosphorylation of LRP6 by CK1 and GSK3ß induces binding of Axin to LRP6 and inhibition of destruction complex function. An important property of Dvl is that it can multimerize through an N-terminal DIX domain (*5*, *6*). The formation of such dynamic aggregates is thought to increase the overall avidity of Dvl for its interaction partners, and mutations in the DIX domain that interfere with multimerization show strongly reduced signaling activity (*5*).

In addition to phosphorylation, Dvl is also regulated by ubiquitylation (*7*–*9*). Ubiquitylation is a versatile posttranslational modification in which specific E3 ubiquitin ligases mediate the addition of ubiquitin molecules—either as single ubiquitin proteins or as ubiquitin polymers—to substrate proteins. Moreover, ubiquitin chains can be linked through different lysines within the ubiquitin sequence, which further increases the functional diversity of this modification. Depending on the type of ubiquitylation, the modified protein is targeted for proteasomal degradation, endocytosed, and routed into the lysosomal degradation pathway, or is affected in its ability to interact with other proteins (*10*). In the case of Dvl, K48-linked polyubiquitylation by kelch-like family member 12 (KLHL12) controls Dvl stability (*7*), but additional ubiquitin modifications may control other aspects of Dvl function (*8*, *11*).

Here, we identified the E3 ubiquitin ligase Huwe1 as an evolutionarily conserved inhibitor of the Wnt/β-catenin signaling pathway. We demonstrate that Huwe1 binds and ubiquitylates Dvl as part of a negative feedback loop in the Wnt signaling pathway.

[1]Hubrecht Institute, Royal Netherlands Academy of Arts and Sciences and University Medical Center Utrecht, Uppsalalaan 8, 3584CT Utrecht, the Netherlands. [2]Institute of Experimental Biology, Faculty of Science, Masaryk University, 61137 Brno, Czech Republic. [3]Institute of Biophysics, Academy of Sciences of the Czech Republic, 61265 Brno, Czech Republic. [4]Cardiff School of Biosciences, Biomedical Sciences Building, Museum Avenue, Cardiff CF10 3AX, UK. [5]Central European Institute of Technology, Masaryk University, 60177 Brno, Czech Republic. [6]National Centre for Biomolecular Research, Faculty of Science, Masaryk University, 61137 Brno, Czech Republic. [7]Department of Functional Genomics, Interfaculty Institute for Genetics and Functional Genomics, Ernst Moritz Arndt University of Greifswald, Friedrich-Ludwig-Jahn-Str. 15, 17487 Greifswald, Germany.
*These authors contributed equally to this work.
†Present address: Department of Pathology, University of Cambridge, Tennis Court Road, Cambridge CB2 1QP, UK.
‡Present address: Department of Clinical Research Medical Oncology, University of Bern, CH-3010 Bern, Switzerland.
§Corresponding author. E-mail: r.korswagen@hubrecht.eu (H.C.K.); bryja@sci.muni.cz (V.B.)

RESULTS

Huwe1/EEL-1 is a negative regulator of Wnt/β-catenin signaling in *Caenorhabditis elegans* and mammalian cells

During larval development in *Caenorhabditis elegans*, EGL-20 (a *C. elegans* Wnt homolog) activates a BAR-1 (a *C. elegans* β-catenin homolog)–dependent Wnt pathway in the QL neuroblasts. Activation of this Wnt pathway induces expression of the homeobox gene *mab-5* in QL and migration of the QL descendant (QL.d) cells toward the posterior (*12*). In the absence of EGL-20 signaling, *mab-5* is not expressed and, as a consequence, the QL.d migrate in the opposite direction, toward the anterior (Fig. 1A). Using the final position of the QL.d as a sensitive measure of β-catenin–dependent Wnt signaling, we performed an RNA interference (RNAi) screen in *C. elegans* that targeted 22 predicted E2 ubiquitin ligases, 173 RING domain E3 ubiquitin ligases, 9 HECT domain E3 ubiquitin ligases, and 34 deubiquitylating enzymes (DUBs) (table S1 and fig. S1A). To screen for both positive and negative regulators of Wnt signaling, we used a *vps-29(tm1320)* mutant background, in which EGL-20 secretion is reduced, resulting in a partially penetrant defect in *mab-5* expression and QL.d migration (*13*). Interfering with positive regulators of EGL-20 signaling enhances this phenotype, whereas knockdown of negative regulators restores posterior QL.d migration in this mutant background (*14*).

We found that knockdown of the HECT domain–containing ubiquitin ligase *eel-1* suppressed the QL.d migration phenotype of *vps-29(tm1320)* mutants (Fig. 1B). Furthermore, using a quantitative single-molecule mRNA fluorescence in situ hybridization (FISH) approach (*15*), we found that loss of *eel-1* significantly increased the expression of the EGL-20 target gene *mab-5* in Q neuroblasts (Fig. 1C), indicating that EEL-1 functions as a negative regulator of EGL-20 signaling.

To investigate the function of EEL-1 in another Wnt-dependent process, we examined vulva formation, in which Wnt/β-catenin signaling plays a permissive role in preventing fusion of the vulva precursor cells (VPCs) with the surrounding hypodermal syncytium (*16*). In hypomorphic mutants of the Wnt secretion factor *mig-14* (the *C. elegans* Wntless homolog), a decrease in Wnt signaling leads to a partially penetrant defect in vulva induction (*17*). RNAi against *eel-1* significantly rescued this defect (Fig. 1D), supporting the notion that EEL-1 functions as a general regulator of Wnt/β-catenin signaling in *C. elegans*.

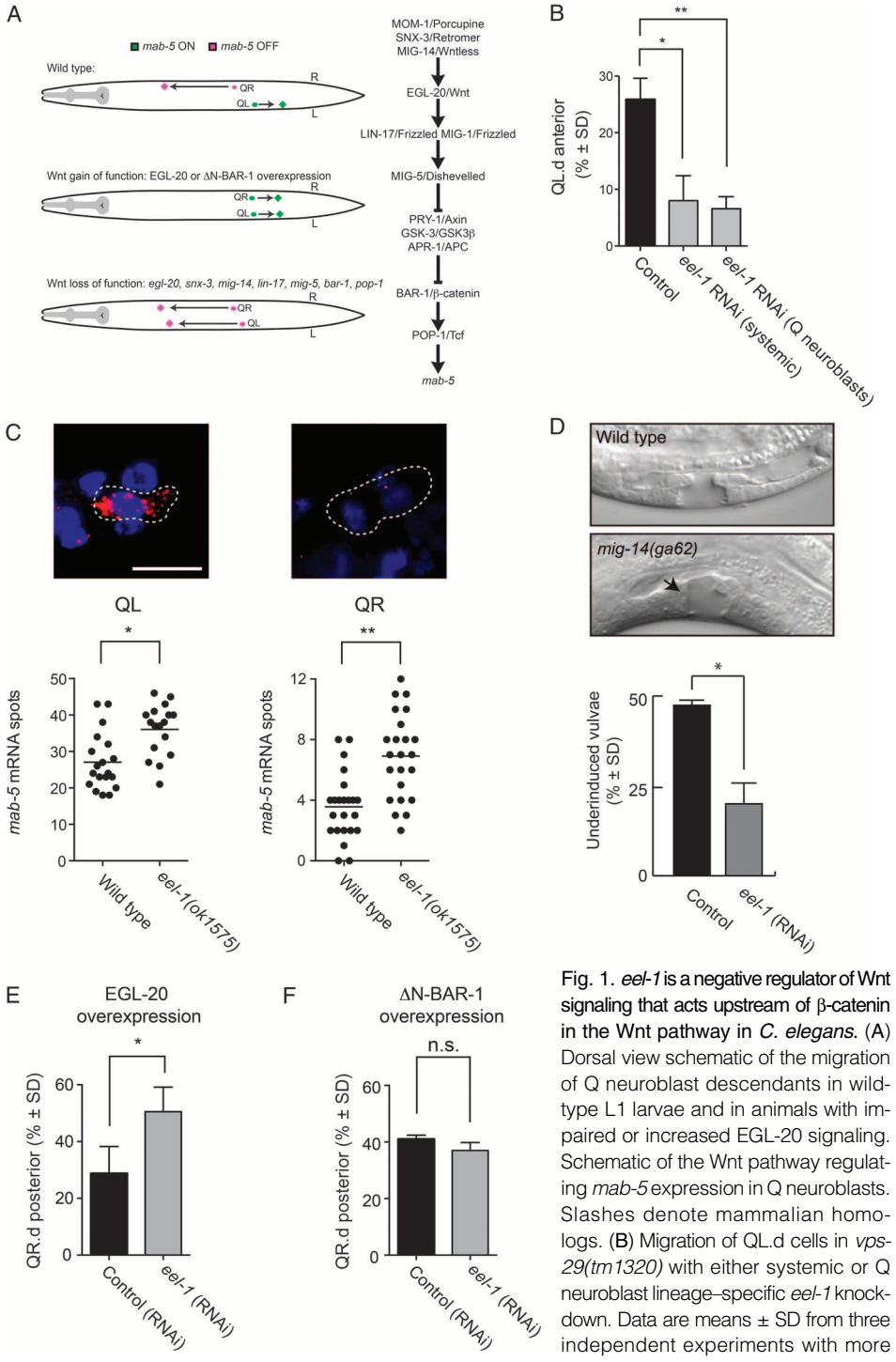

Fig. 1. *eel-1* is a negative regulator of Wnt signaling that acts upstream of β-catenin in the Wnt pathway in *C. elegans*. (**A**) Dorsal view schematic of the migration of Q neuroblast descendants in wild-type L1 larvae and in animals with impaired or increased EGL-20 signaling. Schematic of the Wnt pathway regulating *mab-5* expression in Q neuroblasts. Slashes denote mammalian homologs. (**B**) Migration of QL.d cells in *vps-29(tm1320)* with either systemic or Q neuroblast lineage–specific *eel-1* knockdown. Data are means ± SD from three independent experiments with more than 30 worms each; $*P = 0.0063$, $**P = 0.0037$, Student's *t* test. (**C**) Quantitative single-molecule mRNA FISH showing the expression of the Wnt target gene *mab-5* in QL and QR neuroblasts from wild-type and *eel-1(ok1575)* null mutants. Data are amalgamated from two experiments; $*P = 4.9 \times 10^{-5}$, $**P = 9.6 \times 10^{-4}$, Student's *t* test. Representative QL and QR neuroblasts are from wild-type animals: nuclei (blue), *mab-5* mRNA (red), and Q cells (outlined). Scale bar, 5 μm. (**D**) Effect of *eel-1* RNAi on the vulva defect, indicated by an arrow. Data are means ± SD from four independent experiments with more than 10 animals each; $*P = 0.015$. (**E** and **F**) Effect of *eel-1* RNAi on the response to overexpression of EGL-20 (E) or ΔN-BAR-1 (F). Data are means ± SD from four experiments with more than 30 animals each; $*P = 0.015$, Student's *t* test. n.s., not significant.

To address whether EEL-1 is required in Wnt-responsive cells, we used a tissue-specific RNAi approach to knock down *eel-1* in the Q neuroblast lineage. Similar to systemic RNAi, knockdown of *eel-1* in the Q neuroblasts significantly rescued QL.d migration in the *vps-29* mutant background (Fig. 1B). In contrast, knockdown of *eel-1* in EGL-20–producing cells had no effect (fig. S1B). These results are consistent with a cell-autonomous function of EEL-1 in Wnt-responsive cells.

To determine the position of EEL-1 in the Wnt/β-catenin pathway that regulates *mab-5* expression in the Q neuroblasts, we performed epistasis analysis with loss-of-function mutations in different Wnt pathway components. RNAi against *eel-1* suppressed the QL.d migration phenotype of *vps-29* and *mig-14* mutants, but had no effect in *bar-1* or *pop-1*/TCF mutants (table S2). Together with the cell-autonomous function of EEL-1 in the Q neuroblast lineage, these results place EEL-1 between the Wnt pathway ligand EGL-20 and *bar-1*. This conclusion is further supported by experiments in which we overexpressed EGL-20 or constitutively active BAR-1 (ΔN-BAR-1) (*17*) to induce ectopic expression of *mab-5* in QR and posterior migration of the QR.d. Thus, *eel-1* RNAi strongly enhanced the EGL-20–induced posterior migration of the QR.d (Fig. 1E), whereas no effect was observed when ΔN-BAR-1 was overexpressed (Fig. 1F), consistent with a function of EEL-1 downstream of EGL-20 but upstream of BAR-1. *eel-1* RNAi did not restore QL.d migration in *egl-20* null mutants (table S2), indicating that loss of EEL-1 is not sufficient to activate the EGL-20 pathway in the absence of Wnt ligand.

In parallel to the screen in *C. elegans*, we knocked down Huwe1, the mammalian ortholog of *eel-1*, in human embryonic kidney (HEK) 293T cells stably transfected with a Dvl–estrogen receptor fusion protein and a TOP-luciferase TCF reporter (7DF3 cells) (*18*). We found that knockdown of Huwe1 (Fig. 2B) enhanced the estradiol-dependent activation of the TCF reporter (fig. S2A). This effect was confirmed with nonoverlapping small interfering RNAs (siRNAs) in 7DF3 and U2OS cells (fig. S2, B and C).

Next, we activated the Wnt pathway in HEK293T cells with recombinant Wnt3a by expression of constitutively active N-terminally truncated LRP6 (LRP6ΔN) (*19*), coexpression of Dvl3 and CK1ε (*3*), or expression of constitutively active β-catenin (*20*). Knockdown of Huwe1 (Fig. 2B) increased Wnt reporter activity when the pathway was activated by Wnt3a, LRP6ΔN, or Dvl3 and CK1ε, but not when the pathway was activated by expression of constitutively active β-catenin (Fig. 2, C to F). When we overexpressed a Huwe1 fragment containing the HECT domain [hemagglutinin (HA)–tagged ΔN-Huwe1, encompassing the C-terminal half of the protein from amino acids 2473 to 4374] (*21*), Wnt reporter activity induced by Dvl1 or LRP6ΔN was significantly inhibited, whereas reporter activity induced by β-catenin was not changed (Fig. 2, G to I). As an independent readout for Wnt pathway activity, we assessed the mRNA expression of the Wnt target gene *Axin2* in cells that expressed constitutively active mutants of β-catenin. Huwe1 overexpression did not affect *Axin2* expression in these cells (Fig. 2J). Together with the *C. elegans* data discussed above, these results suggest that Huwe1 functions as an evolutionarily conserved negative regulator of Wnt signaling that acts upstream of β-catenin in the Wnt pathway.

Huwe1 binds Dvl

We obtained further mechanistic insight into the role of Huwe1 in Wnt signaling when we immunoprecipitated endogenous Dvl2 and Dvl3 from mouse embryonic fibroblasts (MEFs) and analyzed the associated proteins

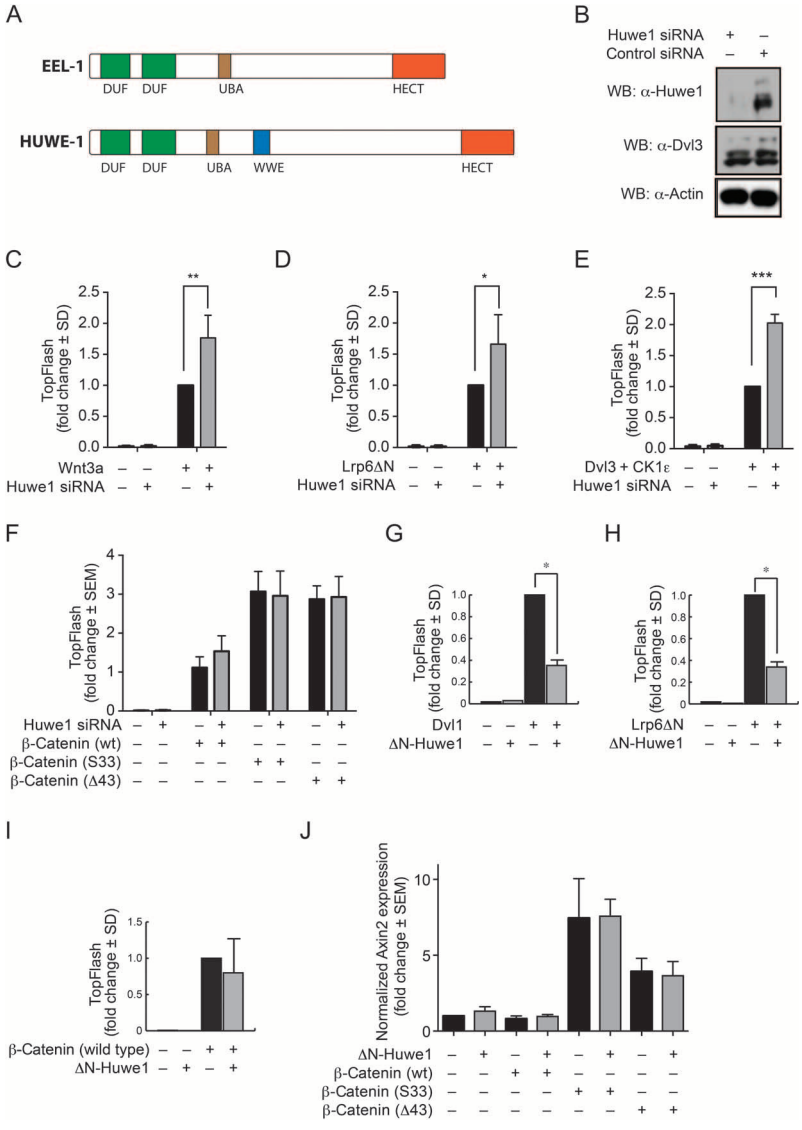

Fig. 2. Huwe1 is a negative regulator of Wnt signaling that acts upstream of β-catenin in the Wnt pathway in mammalian cells. (**A**) Schematic representation of EEL-1 and the human ortholog Huwe1. (**B**) Representative Western blot of Huwe1 knockdown efficiency in HEK293T cells. (**C** to **E**) TopFlash reporter activity in Huwe1 knockdown HEK293T cells that (C) were treated with recombinant Wnt3a, (D) expressed LRP6ΔN, or (E) expressed Dvl3 and CK1ε. Data are means ± SD from three independent experiments; $^{**}P = 0.009$, $^{*}P = 0.04$, $^{***}P = 0.0062$ against controls, Student's *t* test. (**F**) TopFlash reporter activity in Huwe1 knockdown cells that expressed constitutively active β-catenin mutants. Data are means ± SEM from seven experiments. (**G** to **I**) Effect of HA-ΔN-Huwe1 overexpression on TopFlash activity in HEK293T cells expressing (G) Dvl1 ($^{*}P = 0.0022$), (H) LRP6ΔN ($^{*}P = 0.015$), or (I) β-catenin. Data are means ± SD from at least three independent experiments. (**J**) Effect of Huwe1 overexpression on *Axin2* mRNA abundance in cells expressing constitutively active β-catenin mutants. Data are means ± SEM from at least three independent experiments.

by mass spectrometry (MS) (table S3). We discovered that Huwe1 formed a complex with endogenous Dvl2 and Dvl3. To confirm this result, we performed coimmunoprecipitation experiments with antibodies directed against endogenous Huwe1, Dvl2, and Dvl3 and found that Huwe1 can interact with Dvl2 as well as Dvl3 (Fig. 3A). Treatment of cells with Wnt3a conditioned medium (Wnt3a CM) promoted the interaction of endogenous Huwe1 with endogenous Dvl2 and Dvl3 (Fig. 3A). Similar results were obtained with epitope-tagged versions of Dvl1 and ΔN-Huwe1 (fig. S3D). This result indicates that Wnt signaling promotes the interaction between Dvl and Huwe1, but that this interaction does not require the N terminus of Huwe1.

Dvl proteins form dynamic protein assemblies that are visible as distinct punctae within the cytoplasm (*6*). Consistent with the interaction between Huwe1 and Dvl, immunofluorescence experiments using epitope-tagged or fluorescently tagged versions of Huwe1 and Dvl2 or Dvl3 showed that Huwe1, which was diffusely localized throughout the cytoplasm when expressed alone, was recruited to Dvl punctae and colocalized with Dvl2 or Dvl3 when Dvl was coexpressed (Fig. 3B and fig. S3E). An E3 ligase–deficient Huwe1(CA) mutant also colocalized with Dvl in cytoplasmic punctae (Fig. 3B), indicating that the interaction between Huwe1 and Dvl is independent of Huwe1 ligase activity.

To further characterize the interaction between Dvl and Huwe1, we used truncated forms of Dvl1 and Dvl3 to map the domain of Dvl that is required for binding to HA-tagged ΔN-Huwe1. In both cases, we found that a proline-rich region between the PDZ and DEP domains of Dvl appeared to be necessary and sufficient for the interaction between Huwe1 and Dvl1 and Dvl3 (Fig. 3, C and D, and fig. S3, A to C).

One of the earliest events in Wnt pathway activation is the CK1ε-mediated phosphorylation of Dvl (*22*). To address the role of CK1ε in the regulation of the Huwe1-Dvl interaction, we performed coimmunoprecipitation experiments with FLAG-tagged Dvl3 and HA-tagged ΔN-Huwe1 in cells overexpressing CK1ε. CK1ε promoted the Huwe1-Dvl3 interaction, whereas expression of a dominant-negative CK1ε or treatment with the chemical CK1ε inhibitor D4476 (CK1 inhibitor I) or PF-670462 (CK1 inhibitor II) appeared to reduce this interaction (Fig. 3E). Together, these results indicate that Wnt signaling and phosphorylation

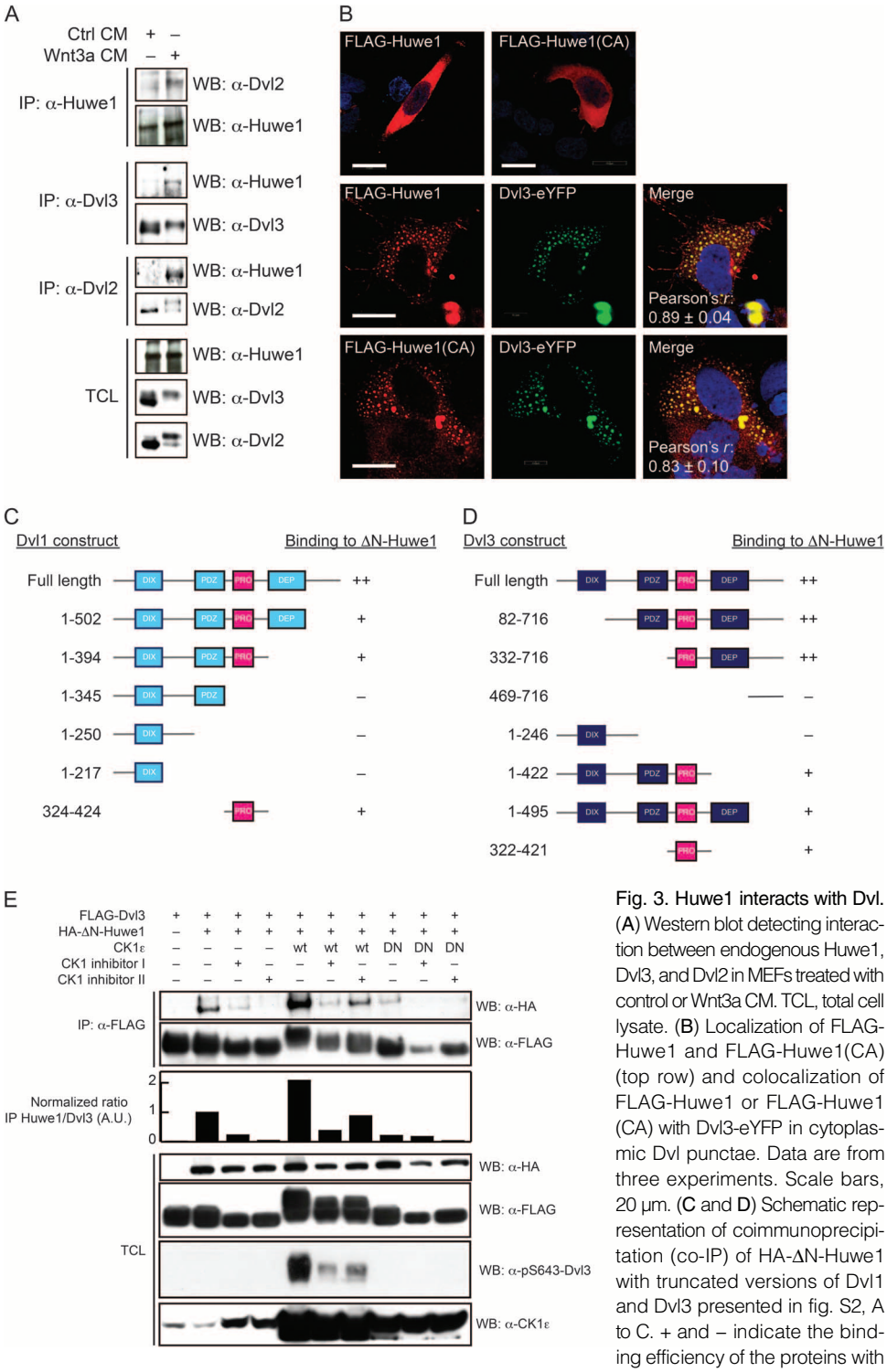

Fig. 3. Huwe1 interacts with Dvl. (**A**) Western blot detecting interaction between endogenous Huwe1, Dvl3, and Dvl2 in MEFs treated with control or Wnt3a CM. TCL, total cell lysate. (**B**) Localization of FLAG-Huwe1 and FLAG-Huwe1(CA) (top row) and colocalization of FLAG-Huwe1 or FLAG-Huwe1 (CA) with Dvl3-eYFP in cytoplasmic Dvl punctae. Data are from three experiments. Scale bars, 20 μm. (**C** and **D**) Schematic representation of coimmunoprecipitation (co-IP) of HA-ΔN-Huwe1 with truncated versions of Dvl1 and Dvl3 presented in fig. S2, A to C. + and – indicate the binding efficiency of the proteins with HA-ΔN-Huwe1. (**E**) Coimmunoprecipitation of HA-ΔN-Huwe1 with FLAG-Dvl3 in HEK293T cells expressing wild-type (wt) or dominant-negative (DN) CK1ε or treated with the chemical CK1ε inhibitor D4476 (I) or PF-670462 (II). The efficiency of CK1-mediated phosphorylation was monitored using a phospho-Ser^{643}-Dvl3 antibody. Blot is representative of three experiments.

of Dvl by CK1ε promote the interaction between Dvl and Huwe1.

Huwe1 promotes the ubiquitylation of Dvl

Huwe1 is a HECT domain E3 ubiquitin ligase that ubiquitylates various substrates and is involved in regulating processes ranging from apoptosis and neuronal differentiation to DNA repair (*21*, *23*–*27*). To investigate whether Huwe1 ubiquitylates Dvl, we coexpressed FLAG-tagged Dvl1 and His-tagged ubiquitin with ΔN-Huwe1 or a catalytically inactive ΔN-Huwe1(CA) mutant (*26*). Western blotting for FLAG-Dvl1 among His-ubiquitin–modified proteins showed that ΔN-Huwe1 promoted the ubiquitylation of Dvl1, whereas ΔN-Huwe1(CA) did not (Fig. 4A). Expression of full-length Huwe1 (but not catalytically inactive full-length Huwe1) appeared to induce the ubiquitylation of Dvl3 as well (fig. S4A). Furthermore, deletion of the proline-rich region of Dvl1 appeared to prevent its Huwe1-dependent ubiquitylation (fig. S4B), indicating that binding of Huwe1 to Dvl is required for its ubiquitylation.

To investigate whether Wnt signaling regulates the Huwe1-mediated ubiquitylation of Dvl, we treated cells with Wnt3a CM before the ubiquitylation assay. Wnt3a CM induced a clear increase in Huwe1-mediated ubiquitylation of FLAG-Dvl1 (Fig. 4B), indicating that the Huwe1-dependent ubiquitylation of Dvl is stimulated by Wnt signaling. Because CK1ε activity promoted the interaction between Dvl and Huwe1 (Fig. 3E), we investigated the effect of CK1ε in the Huwe1-mediated ubiquitylation of Dvl. We found that inhibition of CK1ε reduced FLAG-Dvl1 ubiquitylation in cells expressing ΔN-Huwe1 (Fig. 4C), indicating that CK1ε activity promotes the Huwe1-dependent ubiquitylation of Dvl.

To gain further insight into the functional consequences of Huwe1-mediated ubiquitylation of Dvl, we used an MS-based approach to identify the lysines of Dvl1 that are ubiquitylated by Huwe1. We expressed His-tagged ubiquitin and FLAG-tagged Dvl1, or His-ubiquitin, FLAG-Dvl1, and ΔN-Huwe1, in HEK293T cells. We lysed the cells under denaturing conditions, isolated Dvl by immunoprecipitation, and prepared the samples for MS analysis. The detection of ubiquitylated residues in Dvl1 was based on the characteristic ubiquitin-derived diglycine mass increment of ubiquitylated peptides (114.1 daltons per modified lysine residue) after tryptic digestion. In addition to five lysine residues that were ubiquitylated in the control condition, we found five additional lysine residues that were ubiquitylated when ΔN-Huwe1 was coexpressed (Lys^{34}, Lys^{46}, Lys^{60}, Lys^{69}, and Lys^{412}) (table S4). Most of these lysines were located within the DIX domain of Dvl (Fig. 4D), suggesting that this region is preferentially ubiquitylated by Huwe1. In agreement with this hypothesis, we found that a Dvl1 mutant (DIX7KR, in which the seven lysines in the DIX domain were mutated into arginines) was ubiquitylated with a much lower efficiency by ΔN-Huwe1 than wild-type Dvl1 or a Dvl1 mutant in which the lysines in the PDZ domain (PDZ3KR) were mutated (Fig. 4E). Mutation of the lysines within the DEP domain (DEP6KR) also decreased the amount of Huwe1-dependent ubiquitylation (Fig. 4E). However, given that the DEP domain is dispensable for Wnt/β-catenin signaling (*28*, *29*), the ubiquitylation of the DIX domain is

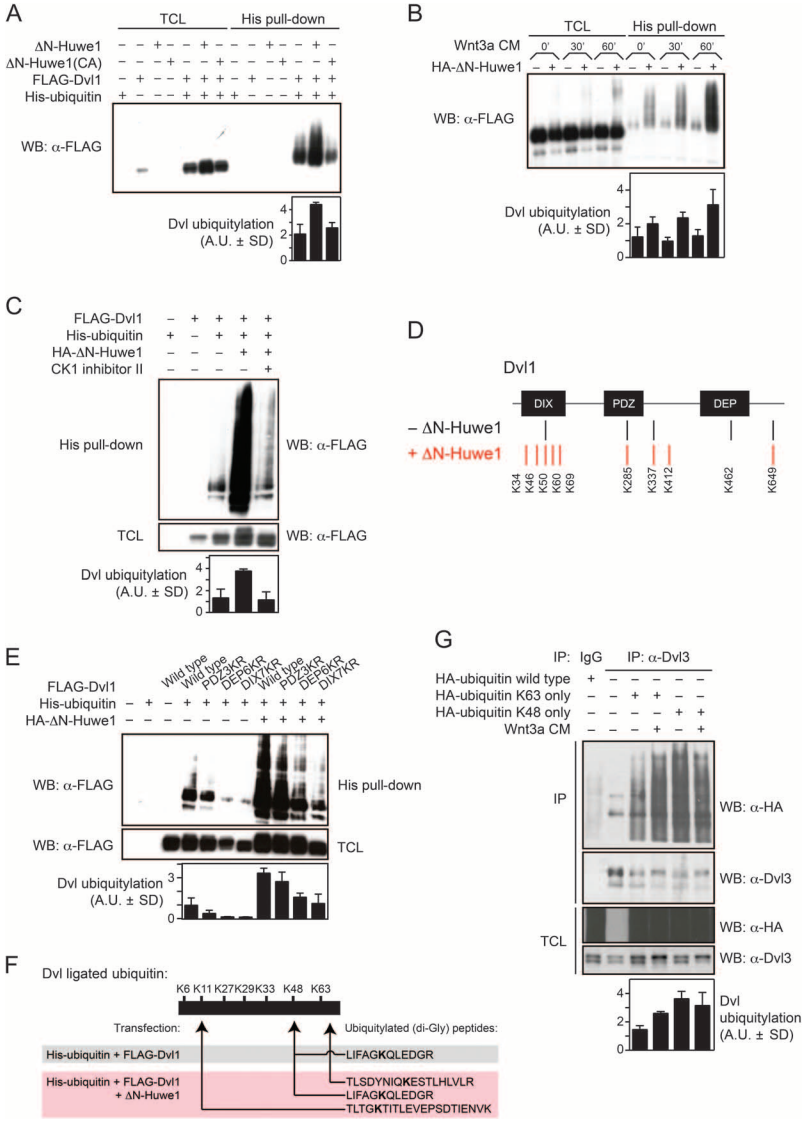

Fig. 4. Huwe1 promotes Dvl ubiquitylation. (**A**) Western blotting for FLAG-Dvl1 after pull-down of His-ubiquitin–modified proteins in HEK293T cells transfected with FLAG-Dvl1, His-ubiquitin, and ΔN-Huwe1 or ΔN-Huwe1(CA). (**B**) Western blotting of lysates from cells transfected as in (A), minus the CA Huwe1 mutant, and treated with control medium or Wnt3a CM for 30 or 60 min before lysis. (**C**) Western blotting of lysates from the cells described in (B) treated with vehicle or PF-670462 (CK1 inhibitor II). (**D**) Schematic representation of ubiquitylated lysine (K) residues of Dvl1 isolated from controls or cells expressing HA-ΔN-Huwe1. (**E**) Western blotting for FLAG-Dvl1 after pull-down of His-ubiquitin–modified proteins in HEK293T cells transfected with HA-ΔN-Huwe1 and FLAG-Dvl1 mutants containing lysine-to-arginine mutants in the PDZ (PDZ3KR), DEP (DEP6KR), or DIX (DIX7KR) domains. (**F**) Schematic representation of ubiquitylated lysine residues of Dvl conjugated to ubiquitin isolated from cells expressing HA-ΔN-Huwe1 or control cells. (**G**) Abundance of ubiquitylation (by HA tag) in endogenous Dvl3 immunoprecipitates from HEK293T cells transfected with wild-type HA-ubiquitin or a HA-ubiquitin mutant that only enables the formation of K63-linked or K48-linked polyubiquitin chains (K63 only and K48 only) and treated with Wnt3a or control CM. Western blotting data are from three independent experiments.

likely to be most relevant for the function of Huwe1 in the Wnt/β-catenin pathway.

The formation of high–molecular weight Dvl species after Huwe1 expression indicates that Huwe1 may promote polyubiquitylation of Dvl. To characterize the ubiquitin chains that are ligated to Dvl, we again used an MS-based approach. This time, we analyzed ubiquitin-derived peptides and determined which lysine residues were ubiquitylated (table S5). In His-ubiquitin– and FLAG-Dvl1–transfected samples, we only detected peptides with the diglycine signature corresponding to Lys^{48} (K48) linkages (Fig. 4F). However, when we expressed ΔN-Huwe1, there were also peptides for K63 and K11 ubiquitin linkages (Fig. 4F), indicating that Huwe1 promotes K63- and K11-linked polyubiquitylation of Dvl. To investigate whether Wnt3a induces the formation of K63-linked polyubiquitin chains on Dvl, we performed a ubiquitylation assay with ubiquitin mutants that only enable the formation of K48- or K63-linked polyubiquitin chains, respectively (*30*). Stimulation with Wnt3a increased the amount of Dvl3 decorated with K63-linked polyubiquitin chains, whereas there was no change in the amount of K48-modified Dvl3 (Fig. 4G). Given the similarity in the ubiquitin modifications induced by Wnt3a and Huwe1, we propose that Huwe1 mediates the Wnt3a-induced K63-linked polyubiquitylation of Dvl.

Huwe1 does not target Dvl for degradation but influences Dvl multimerization

We set out to elucidate the mechanism by which the Huwe1-dependent ubiquitylation of Dvl inhibits Wnt signaling. First, we investigated whether Huwe1 targets Dvl for degradation. We expressed FLAG-Dvl1 in HEK293T cells together with HA-ΔN-Huwe1 or KLHL12, a protein that recruits the Cullin-3 ubiquitin ligase toward Dvl and targets Dvl for proteasomal degradation (*7*). We inhibited protein translation by incubating the cells with cycloheximide and determined FLAG-Dvl1 protein expression and stability by Western blotting. We found no reduction in the amount and stability of FLAG-Dvl1 when HA-ΔN-Huwe1 was expressed (Fig. 5A), but we observed a clear reduction in the amount and stability of FLAG-Dvl when KLHL12 was coexpressed. Additionally, we did not observe increased abundance of endogenous Dvl when we knocked down Huwe1 (Fig. 2B). These observations agree with our finding that ΔN-Huwe1 promotes the formation of K63-linked polyubiquitin chains on Dvl, a modification that in general does not target the substrate protein for proteasomal degradation (*10*).

The formation of DIX domain–dependent multimeric aggregates is essential for Dvl signaling activity (*5*, *31*). Because Huwe1 promoted the ubiquitylation of the DIX domain (Fig. 4, D and E), we investigated whether Huwe1 influences the ability of Dvl to multimerize. To this end, we examined the interaction between different Dvl isoforms by coimmunoprecipitation. Knockdown of Huwe1 increased the coimmunoprecipitation between endogenous Dvl2 and Dvl3 (Fig. 5B), whereas overexpression of HA-tagged ΔN-Huwe1 decreased the coimmunoprecipitation between FLAG-tagged Dvl1 and HA-tagged Dvl2 (Fig. 5D, lanes 1 and 2). Together, these results indicate that Huwe1 inhibited Dvl multimerization. This was supported by the observation that overexpression of HA-tagged ΔN-Huwe1 reduced the interaction between cyan fluorescent protein (CFP)–conjugated Dvl3 and yellow fluorescent protein (YFP)–conjugated Dvl3 in a fluorescence resonance energy transfer (FRET)–based assay (Fig. 5C and fig. S5A).

To investigate whether Huwe1 inhibited Dvl multimerization through ubiquitylation of the DIX domain, we tested the coimmunoprecipitation between HA-tagged Dvl2 and the FLAG-tagged Dvl1-DIX7KR mutant (*8*). This mutant activated the Wnt pathway (assessed by a TopFlash reporter) and localized to punctae in the cytoplasm (fig. S5, B and C), but was only weakly ubiquitylated by Huwe1 (Fig. 4E). We found that overexpression of

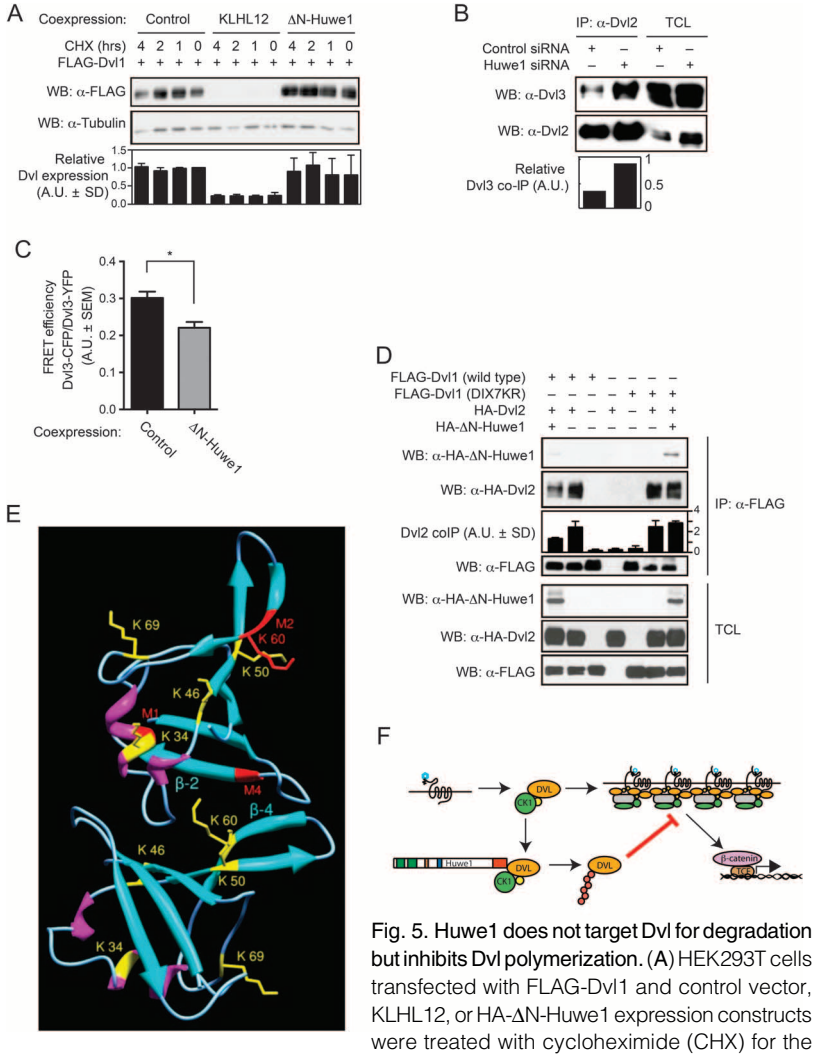

Fig. 5. Huwe1 does not target Dvl for degradation but inhibits Dvl polymerization. (**A**) HEK293T cells transfected with FLAG-Dvl1 and control vector, KLHL12, or HA-ΔN-Huwe1 expression constructs were treated with cycloheximide (CHX) for the indicated time before lysis and FLAG-Dvl1 detection. (**B**) Knockdown of Huwe1 increases coimmunoprecipitation between endogenous Dvl2 and Dvl3. OVCAR-5 cells were transfected with control or Huwe1 siRNA, and endogenous Dvl2 was immunoprecipitated. Dvl3 present in the complex was visualized by Western blotting. (**C**) FRET efficiency between Dvl3-YFP and Dvl3-CFP in HEK293T cells transfected with control or HA-ΔN-Huwe1 expression constructs. For typical FRET images, see fig. S4A. (**D**) Dvl1 was immunoprecipitated with anti-FLAG antibody, and complex composition was determined by Western blotting. (**E**) Structural model of two dimerized DIX domains of Dvl1. Ubiquitylated lysine (K) residues are indicated in yellow. Mutations known to prevent DIX domain polymerization (M1, M2, and M4) are indicated in red; β sheets involved in the head (β2)–tail (β4) interaction are labeled. (**F**) Model of Huwe1 function in Wnt/β-catenin signaling, described in the text. Yellow circles, phosphate; orange circles, ubiquitin; blue hexagons, Wnt.

HA-ΔN-Huwe1 appeared not to decrease the coimmunoprecipitation between FLAG-tagged Dvl1-DIX7KR and HA-tagged Dvl2 (Fig. 5D, lanes 6 and 7), demonstrating that the inhibitory effect of Huwe1 on Dvl multimerization is mediated through ubiquitylation of the DIX domain. Template-based homology modeling of the human Dvl3 DIX domain showed that a number of lysines in the DIX domain that are ubiquitylated by Huwe1 are structurally close, or identical to, residues that have previously been identified as being essential for DIX domain–dependent polymerization (Fig. 5E). Specifically, Lys^{34} (corresponding to Lys^{44} in Dvl2) neighbors a fully conserved phenylalanine, which is mutated in the M1 aggregation mutant (Dvl2-F43S) (*5*). The M1 mutation directly disrupts the "head" side of the polymerization interface. Second, Lys^{60} (corresponding to Lys^{68} in Dvl2) is part of the β4 sheet forming the tail side of the DIX-DIX polymerization interface. Moreover, mutation in a corresponding residue in Dvl2 (K68A, corresponding to the aggregation mutant M2) (*5*) leads to a clear multimerization defect of Dvl2. We therefore propose that ubiquitylation of these residues inhibits DIX domain polymerization through steric effects.

DISCUSSION

Here, we identified the HECT domain–containing E3 ubiquitin ligase Huwe1 as an evolutionarily conserved inhibitor of the Wnt/β-catenin pathway. Our results from epistasis experiments in *C. elegans* and biochemical studies in mammalian cells suggest that Huwe1 acts by inhibiting Dvl signaling activity.

The cytoplasmic protein Dvl functions at a key position in the Wnt/β-catenin pathway, interacting with Fz and Axin to facilitate the formation of signalosomes at the plasma membrane (*2*). The signaling activity of Dvl is promoted by the kinase CK1ε, which in response to Wnt signaling phosphorylates Dvl to induce binding of Dvl to Axin (*3*, *4*, *21*, *31*). We have previously shown that in addition to this activating function, CK1ε also triggers a negative feedback loop that inhibits Wnt signaling, but the mechanism of this inhibition was not determined (*3*). Our results demonstrate that CK1ε induces the binding of Huwe1 to Dvl and provides a molecular mechanism for this inhibition (Fig. 5F).

We found that Huwe1 polyubiquitylated lysine residues within the DIX domain of Dvl. Consistent with our finding that Huwe1 mainly promoted K63- and K11-linked polyubiquitylation of Dvl, Huwe1 did not target Dvl for proteasomal degradation. Instead, we found that Huwe1 inhibited the multimerization of Dvl. As the formation of multimeric complexes is essential for Dvl activity (*5*, *31*), our results are consistent with a model in which Huwe1 inhibits Wnt/β-catenin signaling by preventing Dvl multimerization (Fig. 5F).

Two DUBs—Cyld and USP14—were recently identified that remove K63-linked polyubiquitin chains from Dvl. Cyld removes polyubiquitin (including K63-linked polyubiquitin) chains from the DIX domain of Dvl (*8*). Inhibition of Cyld function and the resulting hyperubiquitylation of Dvl activate Wnt/β-catenin signaling in mammalian cells (*8*). These results support the notion that K63-linked polyubiquitylation is an important regulatory mechanism of Dvl activity, but do not explain why Huwe1 and Cyld both act as inhibitors of Wnt/β-catenin signaling. Cyld and Huwe1 may control the ubiquitylation of different lysine residues within the DIX domain to either promote signaling activity or inhibit signaling by preventing Dvl multimerization. Alternatively, a tight balance in the dynamic addition and removal of K63-linked polyubiquitin chains may be required for the regulation of Dvl activity.

USP14, which also removes K63-linked polyubiquitin chains from Dvl (*32*), was identified as a positive regulator of the Wnt pathway. This observation indicates that it could act as a counterpart to the Huwe1-dependent negative regulation of Wnt signaling. Whether USP14 removes the polyubiquitin chains that are generated by Huwe1, however, remains to be established.

Our study, as well as the work of others, illustrates the importance of ubiquitin-mediated regulation of Dvl signaling in the Wnt pathway. Several E3 ubiquitin ligase systems modify Dvl. Thus, Dvl is targeted for proteasomal degradation by NEDL1, an E3 ligase associated with amyotrophic lateral sclerosis (*33*), by KLHL12, an adaptor protein linking Dvl to the Cullin-3 E3 ubiquitin ligase (*7*), and by Itch, which is a HECT domain E3 ligase (*9*). Thus far, *eel-1* in worms or Huwe1 in mammals represents the only Dvl ubiquitin ligase or DUB with a role in Wnt signaling that is evolutionarily conserved in both vertebrates and invertebrates. This indicates that Huwe1 may represent an ancestral mechanism of Dvl regulation.

Last but not least, Huwe1 was recently identified as an important mediator of Wnt pathway–dependent intestinal tumorigenesis in a mouse transposon insertional mutagenesis screen (*34*). Furthermore, sequence information in the COSMIC database (*35*) shows that Huwe1 is frequently mutated in colon cancer. Our results on the function of Huwe1 as an inhibitor of Wnt/β-catenin signaling—the deregulation of which is the primary cause of intestinal tumorigenesis (*20*)—may provide an important mechanistic explanation for a role of Huwe1 in intestinal cancer.

MATERIALS AND METHODS

C. elegans strains and culture

C. elegans strains were cultured at 20°C under standard conditions as described (*36*). The mutants and transgenes used were *vps-29(tm1320)*, *egl-20(hu105)*, *mig-14(ga62)*, *mig-14(mu71)*, *mig-5(rh147)*, *bar-1(ga80)*, *pop-1(hu9)*, *eel-1(ok1575)*, *muIs32[Pmec-7::gfp]*, *muIs35[Pmec-7::gfp]*, *huIs7[Phs::ΔNbar-1]*, *muIs53[Phs::egl-20]*, *heIs63[Pwrt-2::H2b::gfp; Pwrt2::PH::gfp]*, *huEx273[Pegl-17::eel-1(RNAi)]*, and *huEx274[Pegl-20::eel-1(RNAi)]*.

C. elegans RNAi screen

A list of E2 ubiquitin–conjugating genes, DUBs, RING domain–containing genes, and HECT domain–containing genes was obtained from Kipreos (*37*) (table S1). We isolated RNAi clones targeting these genes from the Vidal or Ahringer RNAi libraries (*38*, *39*). RNAi clones were grown overnight in LB supplemented with ampicillin (50 μg/ml). Bacterial cultures were grown for 3 days on NGM plates supplemented with ampicillin, tetracycline, fungizone, and isopropyl-β-D-thiogalactopyranoside. Two *vps-29(tm1320);muIs32* L4 larvae were placed on the bacterial lawn and allowed to give rise to progeny. The position of the QL.d cells relative to the vulva was scored when the progeny reached the young adult stage (*40*). If RNAi clones modulated the *vps-29* QL.d migration phenotype to >80% or <11%, the RNAi experiment was repeated twice. RNAi clones that consistently enhanced or suppressed the *vps-29* phenotype were considered a hit. The RNAi clones were confirmed by sequencing.

C. elegans tissue-specific RNAi and heat shock experiments

Tissue-specific RNAi was performed as described (*41*). *egl-17* and *egl-20* promoter sequences and a 1.1-kb fragment spanning exon 13 of *eel-1* were amplified from *C. elegans* genomic DNA. The *eel-1* fragment was fused to the promoter fragments in sense and antisense orientations using a polymerase chain reaction (PCR) approach. The PCR products were injected in *vps-29(tm1320); muIs32* at 2.5 ng/μl with *Pmyo2:mCherry* injection marker (7 ng/μl) and pBluescript DNA (200 ng/μl), resulting in transgenic lines *huEx273[Pegl-17::eel-1(RNAi)]* and *huEx274[Pegl-20::eel-1(RNAi)]*.

Embryos isolated by bleaching from *huIs7* or *muIs53* animals grown on *eel-1* or control double-stranded RNA–expressing bacteria were allowed to hatch overnight in M9 buffer. About 100 L1 larvae were heat-shocked in 100 µl of M9 at 33°C for 5 min, and the position of the Q cell descendants AVM and PVM was determined when the animals reached the young adult stage.

Single-molecule mRNA FISH

Single-molecule mRNA FISH was performed as described (*15*). Imaging was performed with a Leica DM6000 microscope equipped with a Leica DFC360FX camera, 100× objective, and Tx2 filter cube. Images were acquired at 1024 × 1024 resolution and 2 × 2 binned before analysis using ImageJ. *mab-5* mRNA spots were manually counted in the Q neuroblasts using *heIs63* as a marker to outline the cells.

Cell culture, plasmids, and transfections

MEFs and HEK293T cells were propagated in Dulbecco's modified Eagle's medium with 10% fetal bovine serum (FBS), 5% L-glutamine, and 5% penicillin/streptomycin. OVCAR-5 cells were grown in RPMI medium with 10% FBS, 5% L-glutamine, and 5% penicillin/streptomycin. Cells were seeded in 24-well plates on coverslips for FRET and immunocytochemistry and 10-cm dishes for immunoprecipitation. Cells were transfected with 2 µl of polyethylenimine per microgram of DNA. Forty-eight hours after transfection, cells were harvested and processed. The following previously described expression constructs were used: Dvl2-Myc (*42*), FLAG-hDvl3 and deletions (*7*), hCK1ε (wild-type and P3 dominant-negative) (*43*), FLAG-mDvl1 deletions and His-ubiquitin lysine mutants (*8*), HA-ubiquitin mutants (*30*), HA-Dvl2 (*31*), HA-ΔN-Huwe1 (*21*), FLAG-Huwe1 and FLAG-Huwe1 (CA) (*27*), β-catenin, S33 β-catenin, Δ43 β-catenin (*20*), Lrp6ΔN (*44*), Super8X TopFlash (*45*), and VSV-KLHL12 (*7*). Dvl3-EYFP, Dvl3-ECFP, and FLAG-Dvl1/Dvl3 Pro-rich were generated by Gateway cloning. Cells were stimulated with mouse rWnt3a (R&D Systems) for 3 hours if not stated otherwise. Control stimulations were done with 0.1% bovine serum albumin (BSA) in phosphate-buffered saline (PBS). CK1ε inhibition was performed with D4476 (Calbiochem) and/or PF-670462 (Tocris) dissolved in dimethyl sulfoxide or with 1 µl of Lipofectamine 2000 (Invitrogen) per well to increase cell penetration.

RNA interference

HEK 293T cells were transfected with Huwe1 endoribonuclease-prepared siRNA (esiRNA) using Lipofectamine 2000. Huwe1 esiRNA (300 ng per well) was mixed with Opti-MEM (Gibco) and 0.5 µl of Lipofectamine 2000 and incubated at room temperature for 30 min, after which the mixture was added to trypsinized cells in 24-well plates. The medium was changed after 12 hours.

Dual luciferase assay

HEK293T cells were seeded in 24-well plates. After 24 hours, cells were transfected with 0.2 µg of Super8X TopFlash construct and 0.2 µg of *Renilla* luciferase construct per well and the indicated expression plasmids. Cells were lysed 24 hours later, and luciferase activity was measured with the Dual-Luciferase Reporter Assay System (Promega) on an MLX luminometer (Dynex Technologies) and normalized by *Renilla* luciferase measurements. Data are shown as means ± SD of at least three independent experiments.

Quantitative reverse transcription PCR

RNA was isolated using TRIzol (Ambion 15596-026) according to the manufacturer's instructions. Reverse transcription was performed with M-MuLV Reverse Transcriptase (Thermo Fisher Scientific), oligo(dT)18 primers (Thermo Fisher Scientific), and 1 µg of RNA for first-strand complementary DNA synthesis. Samples were run as triplicates on a LightCycler 480 II (Roche). β-Actin was used as an internal control. Primers used were human *ACTB* (β-actin; forward: 5′-GATTCCTATGTGGTCGACGAG-3′, reverse: AGGGCTGGGGTGTTGAAGGTCTC) and human *AXIN2* (forward: 5′-TCCATACCGGAGGATGCTGA-3′, reverse: 5′-TTCATACATCGGGAGCACCG-3′).

Antibodies, immunoprecipitation, and Western blotting

Cells were lysed 24 to 48 hours after transfection in NP-40 lysis buffer containing 50 mM tris (pH 7.4), 150 mM NaCl, 1 mM EDTA, 0.5% NP-40, and protease inhibitors (Roche) for 20 min at 4°C and centrifuged at 13,000 rpm for 30 min at 4°C. Supernatant was incubated with the antibodies against mouse monoclonal Dvl3 (Santa Cruz Biotechnology), mouse monoclonal Dvl2 (Santa Cruz Biotechnology), mouse monoclonal FLAG M2 (Sigma), rabbit polyclonal HA (Abcam), or rabbit polyclonal Huwe1 (Bethyl Laboratories) for 30 min on ice followed by incubation with protein G–Sepharose beads (GE Healthcare) overnight at 4°C. Samples were washed five times in NP-40 lysis buffer and analyzed by Western blot with antibodies against mouse monoclonal Myc, goat polyclonal actin, or goat polyclonal Ck1ε (all from Santa Cruz Biotechnology), rabbit polyclonal phospho-Ser^{643}-Dvl3 was raised against peptide HHSLAS(pS)LRSHH (Moravian Biotechnology), or mouse monoclonal α-tubulin (Sigma), followed by horseradish peroxidase–conjugated antibodies against mouse (GE Healthcare) or rabbit (Sigma) immunoglobulin G (IgG).

Immunocytochemistry

HEK293 cells were seeded onto gelatin-coated coverslips in 24-well plates, and transfection was carried out after 24 hours. Transfected cells were fixed after 24 hours in 4% paraformaldehyde for 15 min and blocked with PBTA (3% BSA, 0.25% Triton, 0.01% NaN_3) for 1 hour at room temperature, followed by incubation in primary antibodies overnight at 4°C. Then, cells were washed in PBS; incubated with secondary antibodies conjugated to Alexa 488, Alexa 568, or Alexa 594 (Invitrogen) for 1 hour at room temperature; washed twice with PBS; and mounted in 4′,6-diamidino-2-phenylindole.

Ubiquitylation assay

HEK293T cells were transfected with expression constructs for FLAG-Dvl1, His-ubiquitin, and HA-ΔN-Huwe1; washed 48 hours later in PBS supplemented with 10 mM *N*-ethylmaleimide (NEM); lysed in denaturing guanidium buffer [10 mM tris (pH 8), 0.1 M Na_2HPO_4, 0.1 M NaH_2PO_4, 20 mM imidazole, 6 M guanidium-HCl, and 10 mM β-mercaptoethanol]; and sonicated. Ubiquitylation assays were performed as described using His pull-down (*8*) or a denaturing immunoprecipitation protocol. Samples for denaturing immunoprecipitation were lysed in 0.5% SDS, boiled for 8 min, and sonicated. Then, 1 ml of NP-40 lysis buffer supplemented with protease inhibitors, phosphatase inhibitors, and NEM was added to each sample. Samples were centrifuged at 16.1*g* for 30 min. Sixty microliters of supernatant was reserved for total cell lysate assays, and the rest was used for incubation with the corresponding antibody. Samples were processed and analyzed as in standard immunoprecipitation assays. For His pull-down, the lysate was centrifuged (10 min at 14,000 rpm), and His-tagged proteins were isolated from the supernatant with Ni-NTA beads (Qiagen) for 4 hours at room temperature. The beads were washed in guanidium buffer and three times in ureum buffer before elution of His-tagged proteins in 1× Laemmli sample buffer supplemented with 10 mM tris (pH 7), 0.1 M Na_2HPO_4, 0.1 M NaH_2PO_4, 8 M urea, and 200 mM imidazole.

MS analysis

Samples from the ubiquitylation assays were run on SDS–polyacrylamide gel electrophoresis to separate the ubiquitylated complexes. Gels were

stained with 0.25% Coomassie blue stain (R250). Corresponding one-dimensional (1D) bands were excised and destained, followed by reduction and alkylation. Gel pieces were then subjected to digestion by trypsin for 2 hours at 40°C. Immunoprecipitated Dvl was digested directly in solution.

Liquid chromatography (LC)–MS/MS analyses of peptide mixtures were done using the RSLCnano system connected to an Orbitrap Elite mass spectrometer (Thermo Fisher Scientific). Before LC separation, tryptic digests were concentrated and desalted using a trapping column (100 μm × 30 mm) filled with 3.5-μm X-Bridge BEH 130 C18 sorbent (Waters). After washing with 0.1% formic acid (FA), the peptides were eluted (flow 300 nl/min) from the trapping column onto a Acclaim Pepmap100 C18 analytical column (2-μm particles, 75 μm × 250 mm; Thermo Fisher Scientific) by the following gradient program: mobile phase A—0.1% FA in water; mobile phase B—ACN/methanol/2,2,2-trifluoroethanol (6:3:1, v/v/v) containing 0.1% FA; the gradient elution started at 2% of mobile phase B and increased from 2 to 45% during the first 90 min (11% in the 30th, 25% in the 60th, and 45% in the 90th min), then increased linearly to 95% of mobile phase B in the next 5 min and remained at this state for the next 15 min.

MS data were acquired in a data-dependent strategy with dynamic precursor exclusion selecting up to the top 20 of precursors on the basis of precursor abundance in the survey scan [350 to 1700 mass/charge ratio (*m*/*z*), resolution 120,000]. Low-resolution collision-induced dissociation (CID) MS/MS spectra were acquired in rapid CID scan mode.

FRET analysis

Cells were seeded on gelatin-coated coverslips in 24-well plates and transfected after 24 hours with 0.1 μg of Dvl3-ECFP, 0.1 μg of Dvl3-EYFP, and 0.3 μg of HA-ΔN-Huwe1 using polyethylenimine. Plasmids containing fused EYFP and ECFP together were used as additional controls. The next day, cells were fixed in 4% paraformaldehyde for 15 min and blocked with PBTA (3% BSA, 0.25% Triton, 0.01% NaN_3) for 1 hour at room temperature, followed by incubation in antibodies against HA overnight at 4°C. Cells were then washed in 0.1 M Pipes (pH 6.9) and incubated with Alexa 594–conjugated antibody against rabbit IgG (Invitrogen) at room temperature for 1 hour. Cells were then washed twice with Pipes solution, once with 2 mM $MgCl_2$, and once with EGTA, followed by mounting. FRET between Dvl3-ECFP (donor) and Dvl3-EYFP (acceptor) was measured with a Leica confocal microscope. CFP, YFP, and Alexa 594 were excited using 455-, 514-, and 590-nm lasers, respectively. Region of interest was set on Dvl punctae. Dvl3-YFP punctae were irreversibly bleached for 15 to 30 s. Ratios of donor intensities before and after photobleaching were calculated to obtain FRET efficiencies. To avoid heterogeneity in donor and acceptor expression amounts, we performed experiments three times measuring FRET from 15 to 20 punctae per cell from 4 to 5 cells.

Image quantification

Western blots from three independent experiments were scanned with an Epson perfection 4990 photo scanner. Images were digitally inverted, and band intensities were measured using ImageJ software. Intensities are represented as arbitrary units in each experiment.

3D structure modeling

The 3D model of hDvl3 DIX domain was generated by template-based homology modeling using the program PHYRE2 (*46*), and identified ubiquitin-modified residues and residues corresponding to M1, M2, and M4 DIX mutants (*5*) were mapped and visualized to this 3D model using the CHIMERA program (*47*).

SUPPLEMENTARY MATERIALS

www.sciencesignaling.org/cgi/content/full/7/317/ra26/DC1

Fig. S1. *eel-1* is a negative regulator of Wnt signaling in *C. elegans*.
Fig. S2. *eel-1*/Huwe1 is a negative regulator of Wnt signaling that acts upstream of β-catenin in the Wnt pathway.
Fig. S3. Huwe1 interacts with Dvl and promotes Dvl ubiquitylation.
Fig. S4. Huwe1 promotes Dvl ubiquitylation.
Fig. S5. Huwe1 inhibits Dvl multimerization.
Table S1. List of DUBs, E2 enzymes, and E3 ubiquitin ligases that were screened for enhancement or suppression of the *vps-29(tm1320)*–induced QL.d migration phenotype.
Table S2. Effect of *eel-1*(RNAi) on the EGL-20/Wnt–dependent migration of the QL.d in various Wnt pathway mutants.
Table S3. MS analysis of binding partners of Dvl immunoprecipitated from MEFs.
Table S4. MS analysis of ubiquitylated lysine residues of Dvl1.
Table S5. MS analysis of ubiquitin chain linkage ligated to Dvl1.

REFERENCES AND NOTES

1. B. T. MacDonald, K. Tamai, X. He, Wnt/β-catenin signaling: Components, mechanisms, and diseases. *Dev. Cell* **17**, 9–26 (2009).
2. J. Bilic, Y. L. Huang, G. Davidson, T. Zimmermann, C. M. Cruciat, M. Bienz, C. Niehrs, Wnt induces LRP6 signalosomes and promotes Dishevelled-dependent LRP6 phosphorylation. *Science* **316**, 1619–1622 (2007).
3. O. Bernatik, R. S. Ganji, J. P. Dijksterhuis, P. Konik, I. Cervenka, T. Polonio, P. Krejci, G. Schulte, V. Bryja, Sequential activation and inactivation of Dishevelled in the Wnt/β-catenin pathway by casein kinases. *J. Biol. Chem.* **286**, 10396–10410 (2011).
4. C. M. Cruciat, C. Dolde, R. E. de Groot, B. Ohkawara, C. Reinhard, H. C. Korswagen, C. Niehrs, RNA helicase DDX3 is a regulatory subunit of casein kinase 1 in Wnt–β-catenin signaling. *Science* **339**, 1436–1441 (2013).
5. T. Schwarz-Romond, M. Fiedler, N. Shibata, P. J. Butler, A. Kikuchi, Y. Higuchi, M. Bienz, The DIX domain of Dishevelled confers Wnt signaling by dynamic polymerization. *Nat. Struct. Mol. Biol.* **14**, 484–492 (2007).
6. T. Schwarz-Romond, C. Merrifield, B. J. Nichols, M. Bienz, The Wnt signalling effector Dishevelled forms dynamic protein assemblies rather than stable associations with cytoplasmic vesicles. *J. Cell Sci.* **118**, 5269–5277 (2005).
7. S. Angers, C. J. Thorpe, T. L. Biechele, S. J. Goldenberg, N. Zheng, M. J. MacCoss, R. T. Moon, The KLHL12–Cullin-3 ubiquitin ligase negatively regulates the Wnt–β-catenin pathway by targeting Dishevelled for degradation. *Nat. Cell Biol.* **8**, 348–357 (2006).
8. D. V. F. Tauriello, A. Haegebarth, I. Kuper, M. J. Edelmann, M. Henraat, M. R. Canninga-van Dijk, B. M. Kessler, H. Clevers, M. M. Maurice, Loss of the tumor suppressor CYLD enhances Wnt/β-catenin signaling through K63-linked ubiquitination of Dvl. *Mol. Cell* **37**, 607–619 (2010).
9. W. Wei, M. Li, J. Wang, F. Nie, L. Li, The E3 ubiquitin ligase ITCH negatively regulates canonical Wnt signaling by targeting Dishevelled protein. *Mol. Cell. Biol.* **32**, 3903–3912 (2012).
10. Z. J. Chen, L. J. Sun, Nonproteolytic functions of ubiquitin in cell signaling. *Mol. Cell* **33**, 275–286 (2009).
11. C. Gao, Y. G. Chen, Dishevelled: The hub of Wnt signaling. *Cell. Signal.* **22**, 717–727 (2010).
12. M. Silhankova, H. C. Korswagen, Migration of neuronal cells along the anterior–posterior body axis of *C. elegans*: Wnts are in control. *Curr. Opin. Genet. Dev.* **17**, 320–325 (2007).
13. M. J. Lorenowicz, M. Macurkova, M. Harterink, T. C. Middelkoop, R. de Groot, M. C. Betist, H. C. Korswagen, Inhibition of late endosomal maturation restores Wnt secretion in *Caenorhabditis elegans vps-29* retromer mutants. *Cell. Signal.* **26**, 19–31 (2014).
14. M. Harterink, F. Port, M. J. Lorenowicz, I. J. McGough, M. Silhankova, M. C. Betist, J. R. T. van Weering, R. G. H. P. van Heesbeen, T. C. Middelkoop, K. Basler, P. J. Cullen, H. C. Korswagen, A SNX3-dependent retromer pathway mediates retrograde transport of the Wnt sorting receptor Wntless and is required for Wnt secretion. *Nat. Cell Biol.* **13**, 914–923 (2011).
15. A. Raj, P. Van Den Bogaard, S. A. Rifkin, A. Van Oudenaarden, S. Tyagi, Imaging individual mRNA molecules using multiple singly labeled probes. *Nat. Methods* **5**, 877–879 (2008).
16. T. R. Myers, I. Greenwald, Wnt signal from multiple tissues and *lin-3*/EGF signal from the gonad maintain vulval precursor cell competence in *Caenorhabditis elegans*. *Proc. Natl. Acad. Sci. U.S.A.* **104**, 20368–20373 (2007).
17. J. E. Gleason, H. C. Korswagen, D. M. Eisenmann, Activation of Wnt signaling bypasses the requirement for RTK/Ras signaling during *C. elegans* vulval induction. *Genes Dev.* **16**, 1281–1290 (2002).
18. K. Ewan, B. Pajak, M. Stubbs, H. Todd, O. Barbeau, C. Quevedo, H. Botfield, R. Young, R. Ruddle, L. Samuel, A. Battersby, F. Raynaud, N. Allen, S. Wilson, B. Latinkic, P. Workman, E. McDonald, J. Blagg, W. Aherne, T. Dale, A useful approach to identify novel small-molecule inhibitors of Wnt-dependent transcription. *Cancer Res.* **70**, 5963–5973 (2010).

19. K. Brennan, J. M. Gonzalez-Sancho, L. A. Castelo-Soccio, L. R. Howe, A. M. C. Brown, Truncated mutants of the putative Wnt receptor LRP6/Arrow can stabilize β-catenin independently of Frizzled proteins. *Oncogene* **23**, 4873–4884 (2004).
20. P. J. Morin, A. B. Sparks, V. Korinek, N. Barker, H. Clevers, B. Vogelstein, K. W. Kinzler, Activation of β-catenin-Tcf signaling in colon cancer by mutations in β-catenin or APC. *Science* **275**, 1787–1790 (1997).
21. S. Adhikary, F. Marinoni, A. Hock, E. Hulleman, N. Popov, R. Beier, S. Bernard, M. Quarto, M. Capra, S. Goettig, U. Kogel, M. Scheffner, K. Helin, M. Eilers, The ubiquitin ligase HectH9 regulates transcriptional activation by Myc and is essential for tumor cell proliferation. *Cell* **123**, 409–421 (2005).
22. W. Swiatek, I. C. Tsai, L. Klimowski, A. Pepler, J. Barnette, H. J. Yost, D. M. Virshup, Regulation of casein kinase Iε activity by Wnt signaling. *J. Biol. Chem.* **279**, 13011–13017 (2004).
23. D. Chen, N. Kon, M. Li, W. Zhang, J. Qin, W. Gu, ARF-BP1/Mule is a critical mediator of the ARF tumor suppressor. *Cell* **121**, 1071–1083 (2005).
24. A. J. Ross, M. Li, B. Yu, M. X. Gao, W. B. Derry, The EEL-1 ubiquitin ligase promotes DNA damage-induced germ cell apoptosis in *C. elegans*. *Cell Death Differ.* **18**, 1140–1149 (2011).
25. X. Zhao, D. D' Arca, W. K. Lim, M. Brahmachary, M. S. Carro, T. Ludwig, C. C. Cardo, F. Guillemot, K. Aldape, A. Califano, A. Iavarone, A. Lasorella, The N-Myc-DLL3 cascade is suppressed by the ubiquitin ligase Huwe1 to inhibit proliferation and promote neurogenesis in the developing brain. *Dev. Cell* **17**, 210–221 (2009).
26. X. Zhao, J. I. T. Heng, D. Guardavaccaro, R. Jiang, M. Pagano, F. Guillemot, A. Iavarone, A. Lasorella, The HECT-domain ubiquitin ligase Huwe1 controls neural differentiation and proliferation by destabilizing the N-Myc oncoprotein. *Nat. Cell Biol.* **10**, 643–653 (2008).
27. Q. Zhong, W. Gao, F. Du, X. Wang, Mule/ARF-BP1, a BH3-only E3 ubiquitin ligase, catalyzes the polyubiquitination of Mcl-1 and regulates apoptosis. *Cell* **121**, 1085–1095 (2005).
28. J. D. Axelrod, J. R. Miller, J. M. Shulman, R. T. Moon, N. Perrimon, Differential recruitment of Dishevelled provides signaling specificity in the planar cell polarity and Wingless signaling pathways. *Genes Dev.* **12**, 2610–2622 (1998).
29. M. Boutros, N. Paricio, D. I. Strutt, M. Mlodzik, Dishevelled activates JNK and discriminates between JNK pathways in planar polarity and *wingless* signaling. *Cell* **94**, 109–118 (1998).
30. K. L. Lim, K. C. M. Chew, J. M. M. Tan, C. Wang, K. K. K. Chung, Y. Zhang, Y. Tanaka, W. Smith, S. Engelender, C. a Ross, V. L. Dawson, T. M. Dawson, Parkin mediates nonclassical, proteasomal-independent ubiquitination of synphilin-1: Implications for Lewy body formation. *J. Neurosci.* **25**, 2002–2009 (2005).
31. T. Schwarz-Romond, C. Metcalfe, M. Bienz, Dynamic recruitment of axin by Dishevelled protein assemblies. *J. Cell Sci.* **120**, 2402–2412 (2007).
32. H. Jung, B. G. Kim, W. H. Han, J. H. Lee, J. Y. Cho, W. S. Park, M. M. Maurice, J. K. Han, M. J. Lee, D. Finley, E. H. Jho, Deubiquitination of Dishevelled by Usp14 is required for Wnt signaling. *Oncogenesis* **2**, e64 (2013).
33. K. Miyazaki, T. Fujita, T. Ozaki, C. Kato, Y. Kurose, M. Sakamoto, S. Kato, T. Goto, Y. Itoyama, M. Aoki, A. Nakagawara, NEDL1, a novel ubiquitin-protein isopeptide ligase for Dishevelled-1, targets mutant superoxide dismutase-1. *J. Biol. Chem.* **279**, 11327–11335 (2004).
34. H. N. March, A. G. Rust, N. A. Wright, J. Hoeve, J. De Ridder, M. Eldridge, L. Van Der Weyden, A. Berns, J. Gadiot, A. Uren, R. Kemp, M. J. Arends, L. F. A. Wessels, D. J. Winton, D. J. Adams, Insertional mutagenesis identifies multiple networks of cooperating genes driving intestinal tumorigenesis. *Nat. Genet.* **43**, 1202–1209 (2011).
35. S. A. Forbes, N. Bindal, S. Bamford, C. Cole, C. Y. Kok, D. Beare, M. Jia, R. Shepherd, K. Leung, A. Menzies, J. W. Teague, P. J. Campbell, M. R. Stratton, P. A. Futreal, COSMIC: Mining complete cancer genomes in the Catalogue of Somatic Mutations in Cancer. *Nucleic Acids Res.* **39**, D945–D950 (2011).
36. J. Lewis, J. Fleming, Basic culture methods. *Methods Cell Biol.* **48**, 3–29 (1995).
37. E. T. Kipreos, Ubiquitin-mediated pathways in *C. elegans*. *WormBook* 1–24 (2005).
38. J. F. Rual, J. Ceron, J. Koreth, T. Hao, A. S. Nicot, T. Hirozane-Kishikawa, J. Vandenhaute, S. H. Orkin, D. E. Hill, S. van den Heuvel, M. Vidal, Toward improving *Caenorhabditis elegans* phenome mapping with an ORFeome-based RNAi library. *Genome Res.* **14**, 2162–2168 (2004).
39. R. S. Kamath, A. G. Fraser, Y. Dong, G. Poulin, R. Durbin, M. Gotta, A. Kanapin, N. Le Bot, S. Moreno, M. Sohrmann, D. P. Welchman, P. Zipperlen, J. Ahringer, Systematic functional analysis of the *Caenorhabditis elegans* genome using RNAi. *Nature* **421**, 231–237 (2003).
40. Q. Ch'ng, L. Williams, Y. S. Lie, M. Sym, J. Whangbo, C. Kenyon, Identification of genes that regulate a left-right asymmetric neuronal migration in *Caenorhabditis elegans*. *Genetics* **164**, 1355–1367 (2003).
41. G. Esposito, E. Di Schiavi, C. Bergamasco, P. Bazzicalupo, Efficient and cell specific knockdown of gene function in targeted *C. elegans* neurons. *Gene* **395**, 170–176 (2007).
42. J. S. Lee, A. Ishimoto, S. Yanagawa, Characterization of mouse Dishevelled (Dvl) proteins in Wnt/Wingless signaling pathway. *J. Biol. Chem.* **274**, 21464–21470 (1999).
43. S. Foldynová-Trantírková, P. Sekyrová, K. Tmejová, E. Brumovská, O. Bernatík, W. Blankenfeldt, P. Krejcí, A. Kozubík, T. Dolezal, L. Trantírek, V. Bryja, Breast cancer-specific mutations in CK1ε inhibit Wnt/β-catenin and activate the Wnt/Rac1/JNK and NFAT pathways to decrease cell adhesion and promote cell migration. *Breast Cancer Res.* **12**, R30 (2010).
44. K. Tamai, X. Zeng, C. Liu, X. Zhang, Y. Harada, Z. Chang, X. He, A mechanism for Wnt coreceptor activation. *Mol. Cell* **13**, 149–156 (2004).
45. M. T. Veeman, D. C. Slusarski, A. Kaykas, S. H. Louie, R. T. Moon, Zebrafish prickle, a modulator of noncanonical Wnt/Fz signaling, regulates gastrulation movements. *Curr. Biol.* **13**, 680–685 (2003).
46. L. A. Kelley, M. J. E. Sternberg, Protein structure prediction on the Web: A case study using the Phyre server. *Nat. Protoc.* **4**, 363–371 (2009).
47. E. F. Pettersen, T. D. Goddard, C. C. Huang, G. S. Couch, D. M. Greenblatt, E. C. Meng, T. E. Ferrin, UCSF Chimera—A visualization system for exploratory research and analysis. *J. Comput. Chem.* **25**, 1605–1612 (2004).

Acknowledgments: We thank X. Wang, R. Moon, M. Maurice, A. Fire, S. Yanagawa, M. Bienz, X. He, and M. Eilers for expression vectors, the PRIDE team for data archiving, and the *Caenorhabditis* Genetic Center (University of Minnesota, Minneapolis) for strains. **Funding:** This work was funded by the Dutch Cancer Society (HUBR 2008-4114) (R.E.A.d.G. and H.C.K.), Ministry of Education, Youth, and Sports of the Czech Republic (MSM0021622430), Czech Science Foundation (204/09/H058, 204/09/0498, 13-31488P), EMBO (Installation Grant) (V.B. and O.B.), by the "CEITEC—Central European Institute of Technology" project (CZ.1.05/1.1.00/02.0068) from the European Regional Development Fund, by CEITEC open access project (LM2011020), funded by the Ministry of Education, Youth, and Sports of the Czech Republic under the activity "Projects of major infrastructures for research, development and innovations" (K.Š. and Z.Z.), and by Cancer Research UK, Merck Serono, Breast Cancer Campaign, and Tenovus (T.C.D.). **Author contributions:** R.E.A.d.G. and H.C.K. designed and carried out the *C. elegans* experiments. K.Š., B.L.-L., and T.C.D. performed functional characterization of Huwe1. R.S.G., O.B., R.E.A.d.G., H.C.K., and V.B. designed and carried out cell-based experiments. K.S., Z.Z., and V.M.D. performed MS analysis. R.E.A.d.G., R.S.G., H.C.K., and V.B. wrote the manuscript. **Competing interests:** The authors declare that they have no competing financial interests. **Data and materials availability:** *C. elegans* RNAi data have been submitted to Wormbase (http://www.wormbase.org), accession numbers WBRNAi00094625 to WBRNAi00094815 and are also available at http://www.sci.muni.cz/ofiz/wp-content/uploads/2012/11/De-Groot-2014-Sci-Signal-Suppl.Table-1.pdf. MS data (tables S4 and S5) have been submitted to the PRIDE archive (http://www.ebi.ac.uk/pride/archive/), accession number PXD000781. Data from table S3 are available at http://www.sci.muni.cz/ofiz/wp-content/uploads/2012/11/De-Groot-2014-Sci-Signal-Suppl.Table-3.pdf. Requests for materials should be addressed to H.C.K. and V.B.

Submitted 6 December 2013
Accepted 27 February 2014
Final Publication 18 March 2014
10.1126/scisignal.2004985
Citation: R. E. A. de Groot, R. S. Ganji, O. Bernatik, B. Lloyd-Lewis, K. Seipel, K. Šedová, Z. Zdráhal, V. M. Dhople, T. C. Dale, H. C. Korswagen, V. Bryja, Huwe1-mediated ubiquitylation of dishevelled defines a negative feedback loop in the Wnt signaling pathway. *Sci. Signal.* **7**, ra26 (2014).

Science Signaling

Huwe1-Mediated Ubiquitylation of Dishevelled Defines a Negative Feedback Loop in the Wnt Signaling Pathway

Reinoud E. A. de Groot, Ranjani S. Ganji, Ondrej Bernatik, Bethan Lloyd-Lewis, Katja Seipel, Katerina Sedová, Zbynek Zdráhal, Vishnu M. Dhople, Trevor C. Dale, Hendrik C. Korswagen and Vitezslav Bryja

Sci. Signal. **7** (317), ra26.
DOI: 10.1126/scisignal.2004985

UbiqWNTin Feedback

The Wnt/β-catenin pathway directs the migration of the Q neuroblasts in *Caenorhabditis elegans*. In response to Wnt pathway activation, Dishevelled (Dvl) is activated and the degradation of β-catenin is prevented. Dvl activity is regulated by phosphorylation and ubiquitylation. Using an RNA interference screen targeting ubiquitin ligases and deubiquitylating enzymes, de Groot *et al.* identified the E3 ubiquitin ligase EEL-1 as a Wnt signaling inhibitor that affected Q neuroblast migration. Knockdown of the EEL-1 homolog Huwe1 in human embryonic kidney 293T cells enhanced the activity of the Wnt/β-catenin transcriptional pathway. Huwe1 interacted and colocalized with Dvl. Huwe1 promoted the ubiquitylation of the DIX domain in Dvl and inhibited Dvl multimerization. Thus, Huwe1 functions as an evolutionarily conserved feedback inhibitor of Wnt signaling.

Science Signaling (ISSN 1937-9145) is published by the American Association for the Advancement of Science, 1200 New York Avenue NW, Washington, DC 20005.